Aptamers ISSN: 2514-3247 Aptamers, 2022, Vol 6, 19-27

PROTOCOL

Fluorometry studies of aptamers that bind intrinsically fluorescent ligands: techniques, obstacles and optimizations

Aron A Shoara and Philip E Johnson*

Department of Chemistry and Centre for Research on Biomolecular Interactions, York University, Toronto, Ontario, Canada, M3J 1P3

***Correspondence to:** Philip Johnson, Email: pjohnson@yorku.ca, Tel: 1 416 736 2100 x33119

Received: 22 June 2022 | **Revised:** 03 September 2022 | **Accepted:** 26 September 2022 | **Published:** 26 September 2022

ABSTRACT

Intrinsic fluorescence analysis is a sensitive technique to gain insight about aptamer-small molecule interactions. Employing fluorescence properties of the ligand, the binding affinities of the aptamer-ligand complex can be quantified in the nM to mM range with great accuracy and precision. Here, we present a detection method for aptamer-ligand binding analysis that is based on the inherent fluorescence of the ligand. Further, we discuss how to optimize and resolve some common experimental challenges.

KEYWORDS: Aptamers, fluorometry, fluorescence properties, binding affinity

INTRODUCTION

The exploitation of aptamers in biosensor applications has exposed great sensitivity and often specificity of ligand recognition likely due in large part to the flexible nature of nucleic acids. The cocaine-binding aptamer was originally selected through a systematic evolution of ligands by exponential enrichment (SELEX) method to distinguish cocaine molecules from the metabolites of cocaine(Stojanovic et al, 2000). However, the aptamer's alternative affinity for quinidine alkaloids has enabled this aptamer to be employed as an outstanding experimental binding model for aptamer-small molecule interactions (Pei et al, 2009; Reinstein et al, 2013; Slavkovic et al, 2015).

Common extrinsic fluorescence detection techniques with aptamers involve the addition of a fluorescent or quencher label to the aptamer. However, adding labels can affect the structure of the aptamer (Stojanovic et al, 2000). In this protocol, we develop a detection method for aptamer-ligand binding analysis that is based on the inherent fluorescence of the ligand bound by an aptamer. We describe our methods and protocols that we employed for using ligand fluorescence quenching to quantify the binding affinity of the cocaine-binding aptamer (MN4 construct; Figure 1a) with high sensitivity, accuracy, and precision. We used quinine, cocaine, and tetracycline (Figure 1a) in our studies as they are intrinsically fluorescent ligands, and their binding and structural analyses with nucleic acid molecules have been previously studied (Berens et al, 2001; Shoara et al, 2017; Zhao et al, 2022). We do note that a limitation of using intrinsic fluorescence is that the ligand of interest must be intrinsically fluorescent, and therefore, this technique is limited to a special subset of aptamer-ligand pairs and not all aptamer-ligand combinations. Also, some extreme experimental conditions may reduce or eliminate the inherent fluorescence property of the ligand. For these instances, one can utilize other biophysical methods to study aptamer-ligand binding interactions.

MATERIALS

Instruments

Fluorescence and UV-Visible procedures are performed using Agilent Cary Eclipse and Agilent Cary 100 spectrophotometers. Both spectrophotometers are equipped with xenon flash lamps and linked to Peltier thermostatted cell holders allowing simultaneous temperature control for multiple samples. The chemical and physical properties of cuvettes (*i.e.,* plastic or quartz) used for experiments can impact results. Plastic cuvettes should be avoided when using an organic co-solvent and when working at high temperatures (Nedumpara et al, 2007). The perpendicular

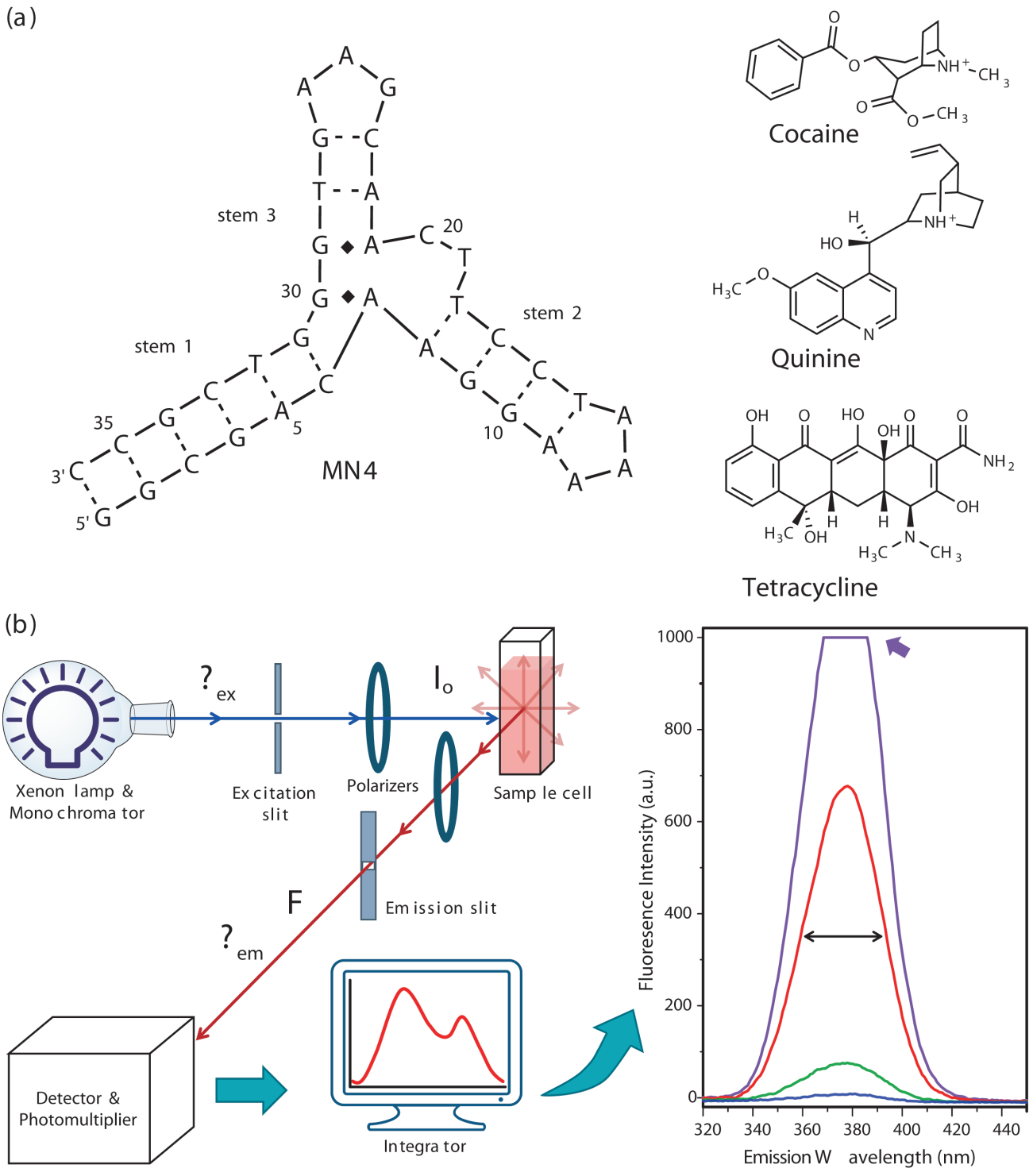

Figure 1. (**a**) Secondary structure of the MN4 cocaine-binding aptamer and chemical structures of the ligands used in this protocol. Dashed lines between nucleotides indicate Watson-Crick base pairing and diamonds show the AG base pairs. Solid lines display the phosphodiester bonds in the backbone of the aptamer. (**b**) Schematic illustration of a fluorescence spectrophotometer. Shown from left to right, a xenon lamp irradiates a sample cell at a known excitation wavelength (λ_{ex}, blue line). The excitation incident light (I_o) goes through an excitation slit. The fluorescence emissions (λ_{em}, red line) from the sample emitted in every direction though only 90° emissions are measured (F). A polarizer is used when polarized fluorescence is measured. Detected emission photons are multiplied and integrated as a function of received emission wavelengths as displayed in the spectra on the right. The superimposed spectra on the right demonstrate the emission peaks of 10µM quinine sample in 0.1 N H_2SO_4 at 25°C with different SBW slit widths: 1.5nm (blue), 2.5nm (green), 5nm (red), and 10nm (purple). Black arrow illustrations NBW of 41nm at 5nm SBW. The SBW/NBW ratio is 0.122 at 350nm excitation. Purple arrow shows the maximum threshold of detection. To obtain an accurate measurement below a SBW/NBW ratio of 0.1 one needs to reduce the fluorophore concentration, PMT voltage, or decrease the slit widths to 2.5nm where NBW is 52nm, and SBW/NBW is 0.048.

profile of excitation and emission beams requires the cuvette to be three- or four-windowed (Figure 1b). Also, one can apply this protocol using multi-cell plate fluorometers (*e.g.*, BioTek Synergy).

Aptamers

DNA and RNA aptamer constructs can be purchased commercially with standard desalting purification.

Buffer materials

Solutions were prepared using distilled deionized (Milli-Q) water (ddH_2O). Since the ionic strength of the solution has a quenching effect on the fluorescence, variation in experimental ionic strength could yield imprecise results. Additionally, some buffer components (*i.e.,* phosphate buffer) have fluorescence quenching effects (Vayá et al, 2010). Materials and manufacturers mentioned in this protocol are stated for transparency purposes, one can use any type or brand of analytical grade reagents.

METHODS

Sample preparation

In preparing samples for binding analysis using intrinsically fluorescent ligands, the following considerations are essential: (*i*) optimal ligand and aptamer concentrations; (*ii*) choice of buffer and ionic strength; (*iii*) organic solvent choice, only if it is necessary to dissolve the ligand. To analyse the dissociation constant (K_d) of a ligand aptamer complex, the detectable ligand must be placed in the cell with the aptamer titrated in. To ensure the ligand is fully saturated with the aptamer, the maximum concentration of aptamer is quantified using:

$$X_{A\bullet L} = [A]^n/(K_d{}^n + [A]^n) \qquad \text{Eq. 1}$$

where $X_{A\bullet L}$ is the fraction of ligand bound, [A] is the starting aptamer concentration and n is the number of binding sites. A suitable starting concentration for a ligand depends on the fluorescence quantum yield of the ligand and the threshold of detection is discussed below.

The aptamer is exchanged three times against 1M NaCl using Amicon-type centrifugal concentrators to remove any substances bound to the aptamer following synthesis and then exchanged 4-6 times against ddH_2O. The stock aptamer concentration should be at least 50-fold higher than the aptamer concentration required to saturate ligand binding. Prior to the binding analysis, the DNA or RNA aptamer constructs should be annealed to favour intramolecular folding. The unbound aptamer samples are incubated in a water bath at 95°C for 3min and then transferred in an ice water bath for 5-10min for fast annealing. For split aptamers, the different strands should be fast annealed, separately. To have low fluorescence quenching interference, it is preferred to degas the ligand and aptamer solutions using sonication or inert gas purging methods (Pedrotti et al, 2000).

Experimental setup

In a fluorescence binding experiment, either the ligand is intrinsically fluorescent, or the aptamer is labelled with a fluorescent dye. To obtain the K_d value of a ligand-aptamer complex, the fluorescent species must be placed in the cell and the total volume of the cell should not be increased by more than 10% of the initial volume. For instance, the ligand must be placed in the cell and the aptamer in the titrant solution if the intrinsic fluorescence of the ligand is utilized. Additionally, the effect of temperature, pH and solvent on the fluorescence intensity and/or binding affinity should be confirmed from literature values or optimized experimentally (Figure 2a). The effect of solvent on the fluorophore may be challenging as some nonpolar ligands are only soluble in mixtures containing an organic solvent such as dimethyl sulfoxide (DMSO) or acetonitrile (ACN). In this case, light absorptivity or fluorescence properties of the organic solvent should be accounted for. Instrumental parameters such as cuvettes, photomultiplier tube (PMT) voltage, excitation and emission slit widths and scan rates should be optimized and kept unchanged to yield the highest sensitivity, accuracy and precision in the results.

Determination of the threshold of detection

To evaluate the precision and accuracy of acquired fluorescence data, it is essential to test the linearity of emission intensities versus ligand concentration by determining the threshold of detection at the lowest and highest concentrations of the ligand. This test is performed to verify the instrument is capable of measuring emission intensities within the range of experimental concentrations.

1. Prepare a fresh stock solution of the ligand in buffer. Note the ligand concentration should be at least 10-fold greater than the highest concentration of the ligand in the experimental design.
2. For each trial, prepare at least 5 ligand samples with different concentrations. The minimum and maximum concentrations should cover the ligand concentration range in the experiment.
3. Using a UV-Vis spectrophotometer, identify the maximum absorbance wavelength of the ligand noting that the maximum excitation wavelength of a fluorophore corresponds to its maximum UV-Vis absorption under the same conditions.
4. Using the fluorimeter, perform an emission scan at a fixed excitation wavelength at 600nm/min, 0.10s averaging time, 1.00nm emission wavelength intervals, and 400-600 Volts PMT.
5. The obtained maximum emission intensities are plotted as a function of ligand concentration and analysed to a linear fit. The signal threshold for concentration limit of detection (C_{LoD}) and limit of quantification (C_{LoQ}) are determined using:

$$C_{LoD} = 3s/m \qquad \text{Eq. 2}$$

$$C_{LoQ} = 10\ s/m \qquad \text{Eq. 3}$$

where s is the residual sum of the vertical intercept (y-intercept) and m is the slope (Long and Winefordner, 1983). Examples of the threshold of detection determination for cocaine and quinine are discussed below.

Photomultiplier optimization

To ensure the best signal-to-noise ratio (S/N), the photomultiplier tube (PMT) voltage variation should be

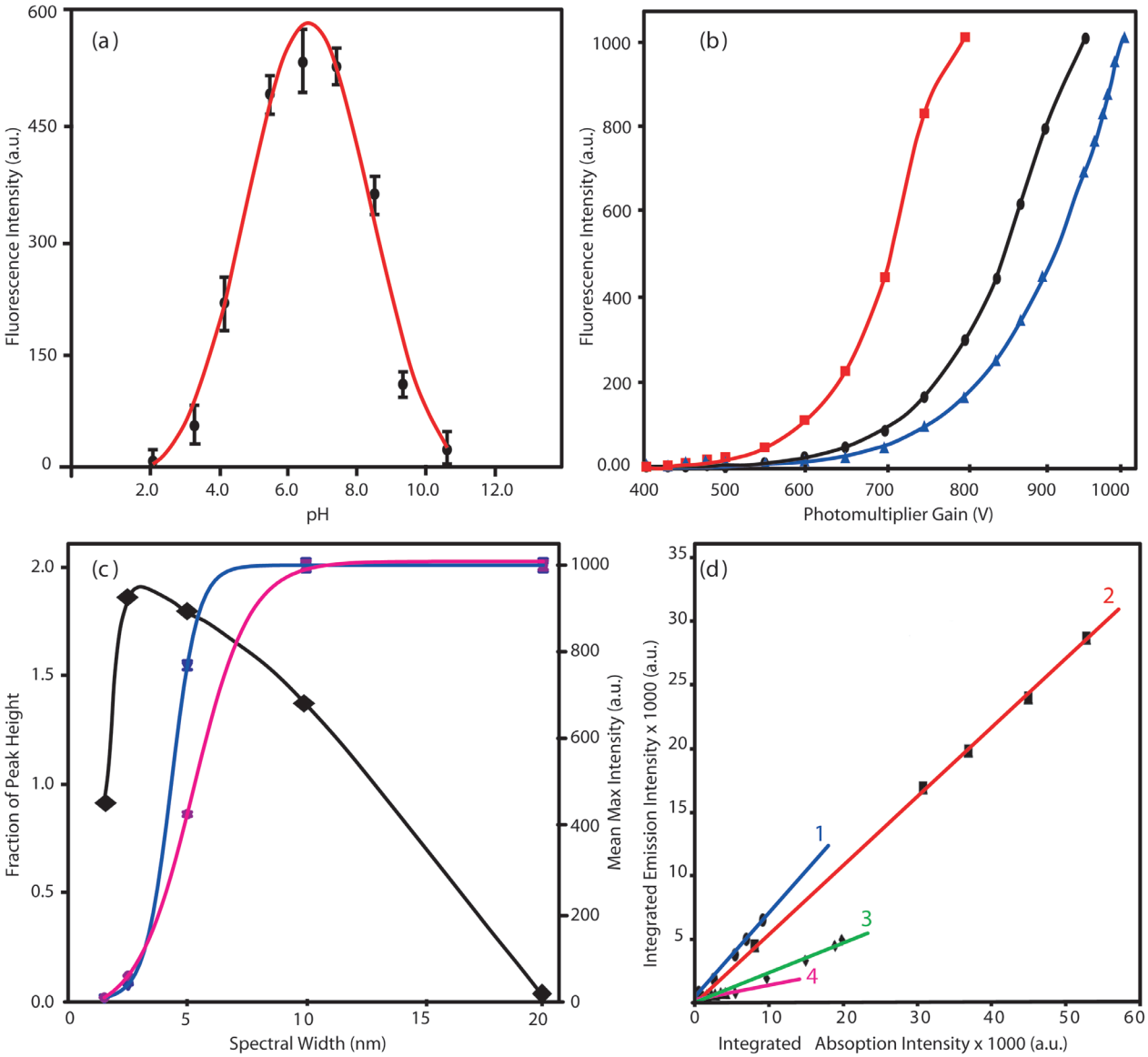

Figure 2. (**a**) The effect of pH change on the fluorescence emission of quinine at 23°C. Fluorescence intensities were fit to a Gaussian curve. Inflection points obtained from the fitted curve (4.83 and 8.49) correspond to pK_a values of quinine. The fitted peak height at pH 6.6 signifies the optimum pH condition (pH 6.6 ± 1) for fluorescence studies of quinine ligand. (**b**) displays the exponential effect of photomultiplier change on the fluorescence intensity of quinine at 23°C. Data acquired at different concentrations of quinine, 0.5µM (red), 0.2µM (black), and 0.1µM (blue). **(c)** shows how the fraction of emission peak height (left vertical axis, black line) changes with effective spectral slit width. Right vertical axis shows how the maximum fluorescence intensity changes with adjusting instrumental bandwidth. Blue and fuchsia lines demonstrate excitation at 235 nm and 330 nm, respectively. Each experiment contains 0.1µM quinine in PBS. Error bars denote one standard deviation of triplicated trials at 23°C. (**d**) displays a comparative analysis of quantum yield measurements. Integrated emission intensities are plotted against integrated absorbance intensities and analysed using a linear regression method. Quinine excited at 330nm (line 1: slope=0.599, R^2=0.9987), quinine excited at 235nm (line 2: slope=0.537, R^2=0.9997), cocaine excited at 232nm (line 3: slope=0.254, R^2=0.9996), and MN4 excited at 260nm (line 4: slope=0.037, R^2=0.9994).

optimized. PMT gain values higher than 800 V reduces the S/N ratio.

1. Set the fluorescence excitation scan mode at the known emission wavelength of the ligand (i.e., 380nm for cocaine and quinine).
2. Using a buffer-only sample, perform fluorescence scans as a negative control.
3. From a concentrated solution of ligand, titrate the ligand into buffer until the intensity of peaks are observed at slightly lower than 1000 au counts.
4. Keeping other parameters constant, obtain fluorescence scans as a function of PMT voltage from 1000V to 400V. Repeat this step to at least 10 different PMT voltage points. Plot emission intensities against PMT values.
5. The observed fluorescence intensity depends on the PMT voltage and excitation wavelength. Figure 2b represents an exponential relationship ($F = 2^{(PMT/100)}$) between the fluorescence intensity of quinine as a function of PMT voltage at three different excitation wavelengths. The optimal PMT is a voltage at which the intensity versus PMT plot holds a linear profile for all ligands in one experiment.

Fluorometer slit width optimization

To have an accurate and precise resolution of fluorescence detection, a monochromatic excitation and emission is preferred. When the irradiated photons pass through monochromator slits, a Gaussian distribution emerges where the spectral bandwidth (SBW) is controlled by the instrument as the width at 50% of the maximum peak intensity (commonly set at 2-10nm). The effective spectral slit width (ESS), the wavelength range covering larger than half of the maximum peak, is often used for SBW, interchangeably. The natural bandwidth (NBW) is the width of an experimentally detected peak at half of the peak height. The ratio of SBW/NBW should equal or be less than 0.100 to have a minimum of 99.5% accuracy of measurement. This ratio shows how accurately the fluorometry detects the true height of the emitted peak. Most scientific spectrophotometers have adjustable slit widths for both excitation and emission monochromators to optimize the instrument for the best resolution (Burgess, 1999).

The high ratio of SBW/NBW generates overlapped peaks and adds stray light rays to the excitation and emission. As a result, a pronounced deviation from the Beer-Lambert law and wider peaks are observed. On the other hand, the low SBW/NBW ratio increases the resolution with a trade-off for reduced sensitivity. The spectrophotometer is expected to resolve 99% of the actual emitted light when the SBW/NBW ratio is 0.125. Figure 2c represents optimization of slit widths for the fluorescence analysis of MN4 and quinine.

Determination of quantum yield

The fluorescence quantum yield (Φ_f) is an intrinsic property of a fluorophore and is the ratio of total emitted photons by the total absorbed photons. The photophysical brightness (*B*) is quantified as the product of the quantum yield and the molar absorption coefficient of the fluorophore at the excitation wavelength (Lakowicz, 1999; Rurack, 2008). Two methods are available in the literature for relative quantum yield analyses: (*i*) single-point, where the emission intensities from a fluorescent ligand and a reference pair at identical concentration and buffer conditions are measured, and (*ii*) comparative methods (Williams et al, 1983). The single-point method estimates Φ_f quickly though it is not considered an accurate method. Here, we show a robust comparative method of quantum yield measurement (Figure 2d).

1. Prepare at least 4 samples of the experimental ligand in the desired buffer conditions and 4 samples of a reference fluorophore solution.
2. Using excitation scan mode, measure fluorescence emission at the excitation wavelength.
3. Plot the integrated fluorescence intensities against the integrated absorbance intensities and perform a linear regression analysis.
4. Repeat steps 1-3 for a reference ligand with known fluorescence quantum yield. Table 1 lists commonly used quantum yield standards (Lakowicz, 1999; Rurack, 2008).
5. The obtained linear slope for the analyte and reference ligands (denoted with subscript R) are compared to determine the fluorescence quantum yield using:

$$\Phi_f = \Phi_R\,(m/m_R)(\eta^2/\eta^2_R) \qquad \text{Eq. 4}$$

where *m* denotes linear slope, and η is refractive index of the solutions (Rurack, 2008).

Table 1. Commonly used fluorescence quantum yield values of reference fluorophores in standard solutions.

Standard compound	Φ_R (%)	Excitation wavelength (nm)	Conditions
Fluorescein	95	496	0.1N NaOH, 22°C
Rhodamine 101	100	450	Ethanol, 25°C
Rhodamine 6G	95	488	Water, 25°C
Rhodamine B	31	514	Water, 25°C
Quinine sulphate	58	350	0.1N H_2SO_4, 22°C
Cyanine 3	4	540	PBS
Cyanine 5	27	620	PBS

Binding affinity determination

To analyse the binding affinities of an equimolar ligand-aptamer complex, the most valid K_d quantification is found using the quadratic function (Eq. 5). We fitted the fluorescence isotherms to a nonlinear regression model defined from the quadratic function and developed in OriginPro 2016:

$$F = F_1 + (F_2 - F_1)\frac{K_d^n}{K_d^n + x^n} \qquad \text{Eq. 5}$$

where *F* is the dependent variable (fluorescence intensity of the ligand), is the independent variable (titrant aptamer concentration), *n* denotes the number of binding events, and F_1 and F_2 are the horizontal and vertical asymptotes, respectively (Shoara et al, 2017).

ANTICIPATED RESULTS

To quantify the K_d value of a ligand-aptamer titration experiment, the maximum emission intensities (or integrated emission peak values) for each titration point is acquired as a function of aptamer concentration. The data should be corrected for any possible light scattering noise or inner-filter effect (described below). As demonstrated in Figure 3a-c, the corrected fluorescence intensities are normalized to have a consistent range of 0-1 in all experimental batches and plotted as against the aptamer concentration and fitted to Eq. 5. For the errors in the K_d, one can either take the standard deviation (SD) of the fitted average values or analyse each trial individually and report the average K_d ± experimental SD.

To characterize the fluorescence properties of the examined ligand, it is essential to test the effect of change in the pH and ionic strength conditions of the experimental design. Any considerable change in pH, ionic strength, viscosity or temperature that influences the quantum yield of a fluorophore can consequently alter the fluorescence detection (Nedumpara et al, 2007). To confirm the pH and ionic strength conditions, where the highest sensitivity of the fluorescence is gained, steady-state fluorescence scans for 7-10 ligand samples can be performed in preferred buffer conditions with a pH range of approximately 2-11. Some ligands exist as diprotonated compounds. For instance, quinine has one aromatic and one aliphatic group offering two pK_a values of 4.2 and 8.3, respectively (Newton and Kluza, 1978). In strong acidic solutions and pH lower

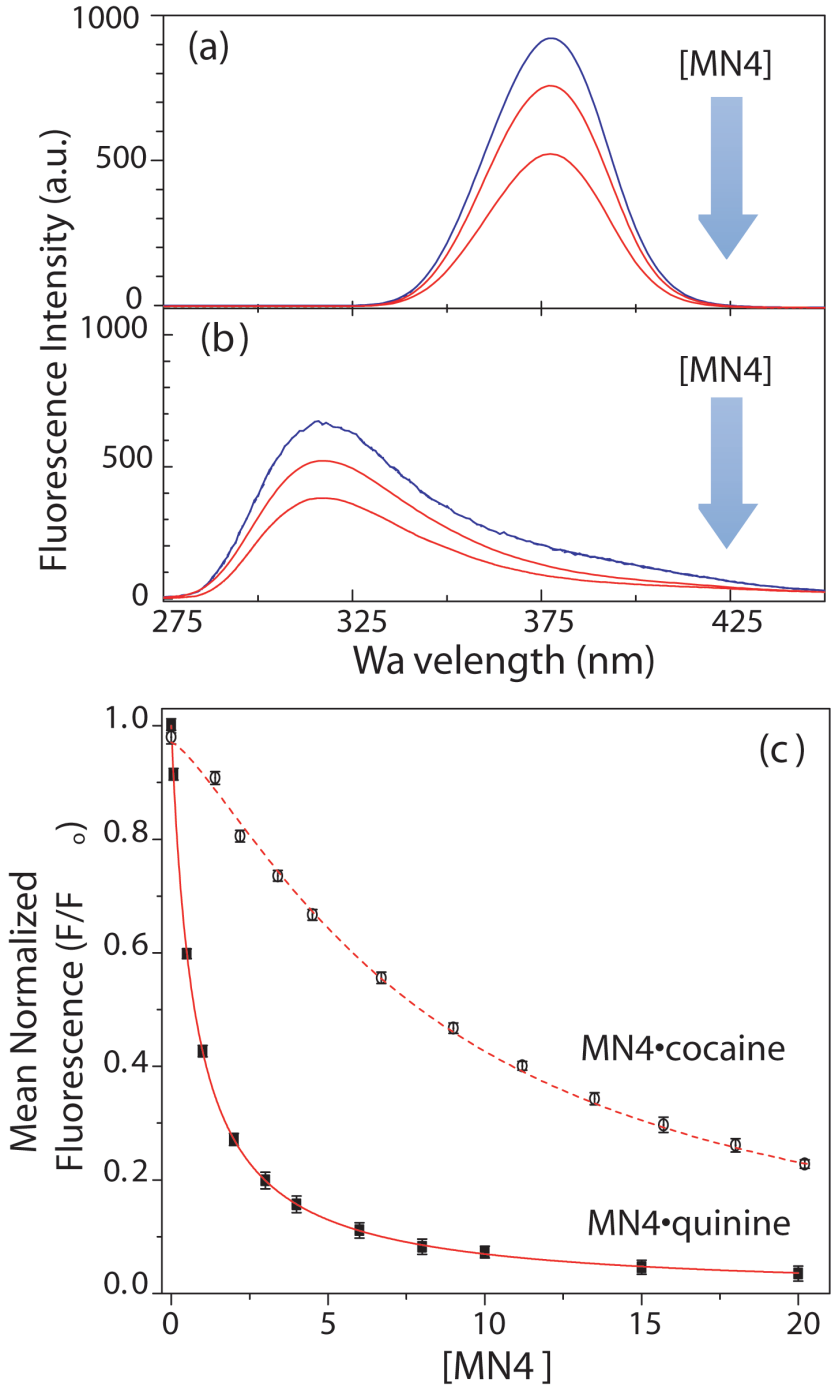

Figure 3. The fluorescence emission spectra of (**a**) quinine and (**b**) cocaine titrated with the MN4 aptamer. Fluorescence scans were carried out in PBS (pH 7.4) at 23°C. Blue spectra denote unbound ligands and red colour denotes spectra following the addition of MN4. Aptamer aliquots quenched the intrinsic fluorescence of 6.0µM quinine excited at 234nm and 4.8µM cocaine excited at 232nm. (**c**) The corrected and normalized relative fraction of fluorescence for each ligand is expressed on the y-axis. F_o and F are inner-filter corrected emission maxima in the absence and presence of the MN4 aptamer, respectively. Each data point signifies an average of 3-6 experiments. Error bars represent one standard deviation. The K_d values were quantified as (0.75 ± 0.01) µM and (7.7 ± 0.1) µM for MN4•quinine and MN4•cocaine titrations, respectively, using Eq. 5.

than 4.0, quinine is fully protonated, and its fluorescence is quenched as the excited state energy is converted internally. Also, the intensity of quinine fluorescence quenches as the ionic strength is increased or pH is higher than 9. The acquired pK_a values (4.83 and 8.49) agreed with available pK_a values of quinine using alternative techniques (Figure 2a).

As the spectral bandwidth increases, the signal resolution is reduced. Figure 1b shows how the ratio of SBW/NBW is quantified to 0.082 at 5nm slit width at 235nm excitation wavelength and 10nm at 335nm excitation wavelength. Obtaining a ratio below 0.1 signifies an accurate measurement (>99.5%) at constant temperature and PMT voltage.

CRITICAL PARAMETERS AND TROUBLESHOOTING

It is possible that detected emission counts are higher than the maximum threshold of 1000au. To resolve this issue, changing one or a combination of the following parameters would be useful: reducing ligand concentration, length of the light path, PMT voltage, excitation slit widths, or increasing the temperature is advised.

In case the fluorescence intensity of the least concentrated ligand sample is found to be as low as the scattering intensities of the buffer, increasing the length of the light path, excitation slit widths, or reducing the temperature can resolve the problem. The optimal bandwidth for an analysis should not necessarily be 1.0nm, though a narrow spectral bandwidth improves the resolution of peaks that are emitted close to each other. If the analyte has low quantum yield, one or a combination of the following adjustments enhances the detection: increasing the excitation slit width, reducing the length of light path, reducing temperature, or the ionic strength. As shown in Figure 2c for quinine emission, the fraction of peak height (resolution) is reduced with the spectral bandwidth increasing from 2.5nm.

Quantum yield is an intrinsic property of a ligand. Thus, Φ_f is independent of the ligand concentration or instrument parameters. However, the ligand concentration needs to be within the linear range of Beer-Lambert law and the instrument parameters should be kept constant throughout the experiment. Any significant change in the pH, ionic strength and refractive index (η) consequently alters Φ_f (Lakowicz, 1999). Figure 2d illustrates a comparative analysis of quantum yield measurements for quinine, cocaine and the MN4 aptamer.

The desired experimental temperature is determined by the aptamer stability, ligand thermolability and instrument limits keeping in mind that binding affinities are temperature dependent (Slavkovic and Johnson, 2018). The temperature can typically be set between -10°C to 120°C with 0.1°C resolution and cell temperature variation of ±0.05°C.

The total number of sample titrations should be uniformly distributed across the concentration range studied to get a precise binding analysis. If one-binding process is anticipated for the aptamer-ligand complex, the titration volume should be chosen such that aptamer to ligand ratio is 1:1 in the middle of the binding titration curve.

Considering nucleotides are weakly fluorescent, measuring the background fluorescence signals from the titration of the aptamer into a blank buffer is essential to confirm the changes in the observed fluorescence was specifically due to ligand-aptamer interactions and not scattering effects (Figure 4b). If the ligand is excited at any wavelengths below ~330nm, where nucleotides absorb UV light, the loss of excitation and emission photons due to the inner-filter effect should be compensated as:

$$F = F_{obs}[10^{(A_{ex}+A_{em})l/2})] \quad \text{Eq. 6}$$

where F is the corrected fluorescence intensity, F_{obs} is the observed intensity *in the absence of the* inner-filter effect, A_{ex} and A_{em} are the absorbance values of the aptamer, or any other light absorbing components, at the excitation and emission wavelengths of the ligand, respectively, and ℓ is the length of the light path (Shoara et al, 2017). Additionally, performing a negative control experiment using a non-binding aptamer with comparable extinction coefficient as the analysed aptamer is highly recommended.

Preliminary data analysis can be performed with the software supplied by the manufacturer (*i.e.,* Eclipse-Bio) or exported to more advanced data analysis software packages (*i.e.,* MATLAB, OriginPro, SigmaPlot). An important setback that can be experienced at micro- or nanomolar concentration scales of ligands is the presence of light scattering spikes in the baseline. Main scattering signals accounted in fluorescence spectrometry of solutions are (*i*) the first and second orders Rayleigh, (*ii*) Tyndall, (*iii*) Raman, which appear depending on the excitation wavelength (Figure 4a). Tyndall scattering is caused by solid particle residues (*i.e.,* dust), which can be eliminated applying a nanopore membrane filtration. The Rayleigh scattering signals appear at the same excitation wavelength and 2x the excitation wavelength. The Raman scattering wavelength of aqueous solutions is attributed to the symmetrical vibrational energy (Price et al, 1962). The mathematical relationship between the excitation wavelength (l_{ex}) and the anticipated Raman scattering signal (λ_R) is expressed as:

$$1/\lambda_R = 1/\lambda_{ex} - 3400\ cm^{-1} \quad \text{Eq. 7}$$

To eliminate the effect of scattering signals, one can change the excitation wavelength to a lower range of excitable wavelengths and adjust the emission scan wavelength range outside the scattering signal. Alternatively, one can subtract the fluorescence intensity of a buffer blank from experimental samples or normalize the observed fluorescence intensity with respect to scattering signals (Li et al, 2000). Figure 4a and b shows anticipated scattering signals with respect to fluorescence emissions of cocaine and tetracycline titrating with the MN4 aptamer. Also, two examples of the threshold of detection determination for cocaine and quinine are demonstrated in Figures 4c and d.

More complicated binding models such as two-site independent binding, sequential binding, and Förster resonance energy transfer (FRET) can also be analysed upon modification of aptamer. Data fitting to more complicated models is beyond the scope of this article and readers are referred to several excellent references (Freiburger et al, 2009; Freire et al, 2009).

ACKNOWLEDGEMENTS

This research is supported by the Natural Sciences and Engineering Research Council (NSERC) of Canada. We thank Logan Donaldson (York University) for the use of the fluorescence spectrophotometer. We also thank all past and present lab members for useful discussions about fluorescence spectrophotometry and aptamer studies.

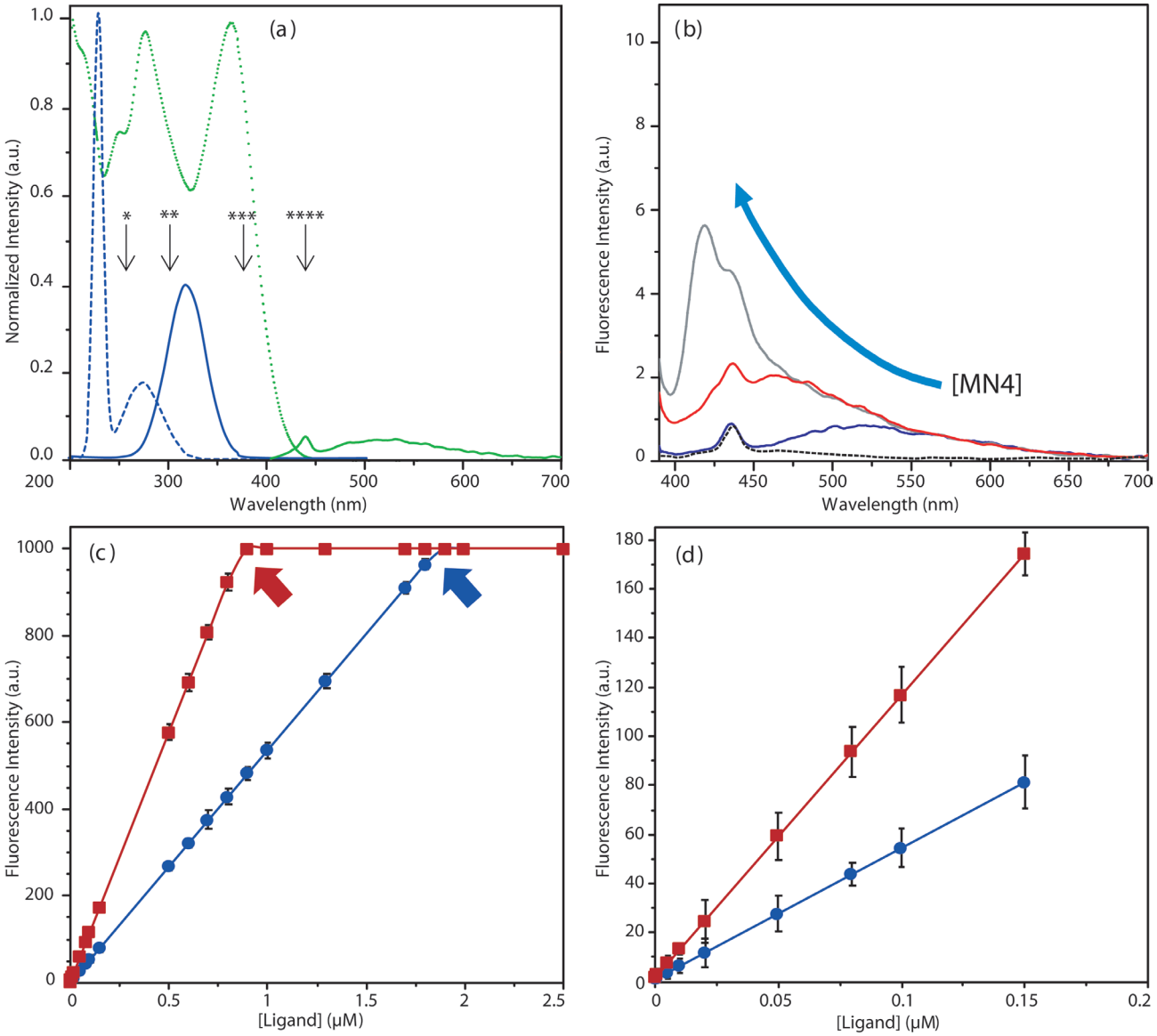

Figure 4. Fluorescence spectra of ligands with respect to light scattering signals and detection limits. (**a**) Excitation spectra are denoted as dashed lines, and emission spectra are shown in solid lines. Blue lines represent the spectra of cocaine, and green lines are for tetracycline in PBS at 25°C. Asterisks denotes anticipated Raman scattering signals in aqueous solutions when excited at 230-235nm (*), 275nm (**), 335nm (***), and 360-365nm (****). (**b**) shows how light scattering can negatively influence the fluorescence emission of tetracycline titrated with MN4. As tetracycline interacts with the aptamer, the emission intensities are enhanced though the emission is near scattering light (blue arrow) observed at ~440nm in a blank PBS sample (black dashed), 0.9μM tetracycline in PBS (blue), 0.9μM tetracycline titrated with 1μM MN4 (red), and 5μM MN4 (grey). (**c**) demonstrates an example of the threshold of detection comparison for cocaine (*blue*) and quinine (*red*) in PBS at 25°C. Arrows show the maximum thresholds of detection. (**d**) exhibits a zoomed view of 0 to 0.2μM ligand concentration from data in (**c**) to show the minimum thresholds of detection. The fitted linear regression values quantified as for cocaine (blue) and for quinine (red). Residual sums of the vertical intercept (y-intercept) values are acquired as ±109.9 for cocaine (blue) and ±103.6 for quinine (red). The minimum thresholds of detection are calculated as = 0.6μM for cocaine and = 0.3μM for quinine using Eq. 2.

COMPETING INTERESTS

None declared.

LIST OF ABBREVIATIONS

au: arbitrary unit
C_{LoD}: concentration limit of detection
C_{LoQ}: concentration limit of quantification
ESS: effective spectral slit width
K_d: dissociation equilibrium constant
NBW: natural bandwidth
PMT: photomultiplier tube
PBS: phosphate-buffered saline
Φ: fluorescence quantum yield
η: refractive index
SBW: spectral bandwidth

REFERENCES

Berens C, Thain A and Schroeder R. 2001. A tetracycline-binding RNA aptamer. Bioorganic & Medicinal Chemistry, 9, 2549-2556.

Burgess CFTUSG (1999) Standards and best practice in absorption spectrometry. Blackwell Science, Oxford; Malden, Mass.

Freiburger LA, Auclair K and Mittermaier AK. 2009. Elucidating protein binding mechanisms by variable-c ITC. ChemBioChem, 10, 2871-2873.

Freire E, Schon A and Velazquez-Campoy A. 2009. Isothermal titration calorimetry: general formalism using binding polynomials. Methods Enzymol, 455, 127-155.

Lakowicz JR (1999) Principles of Fluorescence Spectroscopy. 2 edn. Springer. doi:10.1007/978-0-387-46312-4

Li Y-Q, Qian F and Li Z. 2000. Reduction of second-order scattering interference by variable-angle synchronous luminescence spectroscopy. Chem J Internet, 2, 29-36.

Long GL and Winefordner JD. 1983. Limit of Detection A Closer Look at the IUPAC Definition. Analytical chemistry, 55, 712A-724A.

Nedumpara RJ, J TK, K JV, Girijavallabhan CP, Nampoori VPN and Radhakrishnan P. 2007. Study of solvent effect in laser emission from Coumarin 540 dye solution. Appl Opt, 46, 4786-4792.

Newton DW and Kluza RB. 1978. pKa Values of Medicinal Compounds in Pharmacy Practice. Drug Intelligence & Clinical Pharmacy, 12, 546-554.

Pedrotti JJ, Lima S, Coichev N and Gutz IGR. 2000. Overcoming oxygen quenching in fluorescence spectrometry with a highly efficient in-line degassing device interfaced with a flow cell. Anal Chim Acta, 422, 131-137.

Pei R, Shen A, Olah MJ, Stefanovic D, Worgall T and Stojanovic MN. 2009. High-resolution cross-reactive array for alkaloids. Chem Commun, 3193-3195.

Price JM, Kaihara M and Howerton HK. 1962. Influence of Scattering on Fluorescence Spectra of Dilute Solutions Obtained with the Aminco–Bowman Spectrophotofluorometer. Appl Opt, 1, 521-533.

Reinstein O, Yoo M, Han C et al. 2013. Quinine binding by the cocaine-binding aptamer. Thermodynamic and hydrodynamic analysis of high-affinity binding of an off-target ligand. Biochemistry, 52, 8652-8662.

Rurack K (2008) Fluorescence Quantum Yields: Methods of Determination and Standards. In: Resch-Genger U (ed) Standardization and Quality Assurance in Fluorescence Measurements I: Techniques. Springer Berlin Heidelberg, Berlin, Heidelberg, pp 101-145.

Shoara AA, Slavkovic S, Donaldson LW and Johnson PE. 2017. Analysis of the Interaction between the Cocaine-Binding Aptamer and its Ligands using Fluorescence Spectroscopy. Can J Chem, 95, 1253-1260.

Slavkovic S, Altunisik M, Reinstein O and Johnson PE. 2015. Structure-affinity relationship of the cocaine-binding aptamer with quinine derivatives. Bioorg Med Chem, 23, 2593-2597.

Slavkovic S and Johnson PE. 2018. Isothermal titration calorimetry studies of aptamer-small molecule interctions: practicalaties and pitfalls. Aptamers, 2, 45-51.

Stojanovic MN, de Prada P and Landry DW. 2000. Fluorescent sensors based on aptamer self-assembly. J Am Chem Soc, 122, 11547-11548.

Vayá I, Gustavsson T, Miannay F-A, Douki T and Markovitsi D. 2010. Fluorescence of Natural DNA: From the Femtosecond to the Nanosecond Time Scales. J Am Chem Soc, 132, 11834-11835.

Williams ATR, Winfield SA and Miller JN. 1983. Relative fluorescence quantum yields using a computer-controlled luminescence spectrometer. Analyst, 108, 1067-1071.

Zhao Y, Ong S, Chen Y, Jimmy Huang P-J and Liu J. 2022. Label-free and Dye-free Fluorescent Sensing of Tetracyclines Using a Capture-Selected DNA Aptamer. Anal Chem, 94, 10175-10182.